Published in final edited form as:

Cell. 2015 November 19; 163(5): 1191–1203. doi:10.1016/j.cell.2015.10.074.

Descending Command Neurons in the Brainstem that Halt Locomotion

Julien Bouvier[1,2,4,*], **Vittorio Caggiano**[1,4], **Roberto Leiras**[1], **Vanessa Caldeira**[1], **Carmelo Bellardita**[1], **Kira Balueva**[3], **Andrea Fuchs**[1], and **Ole Kiehn**[1,*]

[1]Mammalian Locomotor Laboratory, Department of Neuroscience, Karolinska Institutet, 17177 Stockholm, Sweden

[2]Paris-Saclay Institute of Neuroscience, UMR 9197 - CNRS and Université-Paris 11, 91190 Gif-sur-Yvette, France

[3]Institute of Physiology, Christian Albrechts University of Kiel, 24098 Kiel, Germany

SUMMARY

The episodic nature of locomotion is thought to be controlled by descending inputs from the brainstem. Most studies have largely attributed this control to initiating excitatory signals, but little is known about putative commands that may specifically determine locomotor offset. To link identifiable brainstem populations to a potential locomotor stop signal, we used developmental genetics and considered a discrete neuronal population in the reticular formation: the V2a neurons. We find that those neurons constitute a major excitatory pathway to locomotor areas of the ventral spinal cord. Selective activation of V2a neurons of the rostral medulla stops ongoing locomotor activity, owing to an inhibition of premotor locomotor networks in the spinal cord. Moreover, inactivation of such neurons decreases spontaneous stopping in vivo. Therefore, the V2a “stop neurons” represent a glutamatergic descending pathway that favors immobility and may thus help control the episodic nature of locomotion.

Graphical abstract

[*]Correspondence: julien.bouvier@inaf.cnrs-gif.fr (J.B.), ole.kiehn@ki.se (O.K.).
[4]Co-first author

SUPPLEMENTAL INFORMATION

Supplemental Information includes Supplemental Experimental Procedures, seven figures, and three movies and can be found with this article online at http://dx.doi.org/10.1016/j.cell.2015.10.074.

AUTHOR CONTRIBUTIONS

J.B. and O.K. conceived the in vitro study. O.K. and V. Caggiano conceived the in vivo study with contributions from R.L. and J.B. J.B. performed anatomical investigations, viral tracings, in vitro recordings, and analyzed data. V. Caggiano and R.L. performed in vivo experiments and analyzed data. C.B. contributed to spinal injections and to locomotor gait analysis. V. Caldeira carried out fluorescent in situ hybridizations. A.F. performed whole-cell recordings of transfected neurons. K.B. produced the TeLC-coding virus. J.B. and O.K. wrote the paper with contributions of all authors. O.K. supervised all aspects of the work and provided the funding of the work.

We declare no conflict of interest regarding this work.

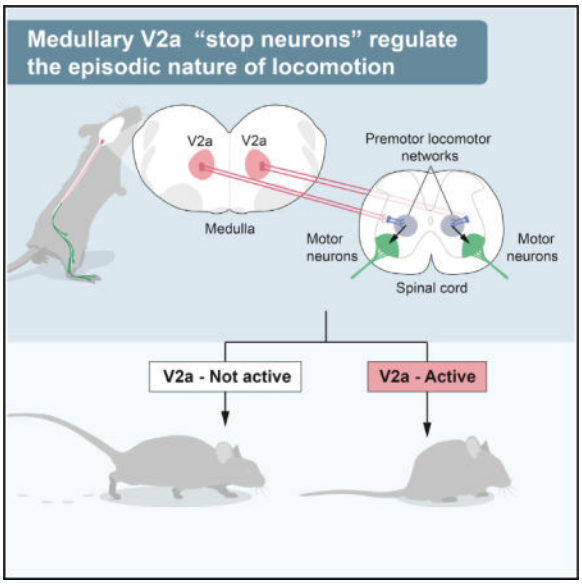

INTRODUCTION

Locomotion is one of many motor acts that the brain controls. It is a rhythmic and episodic behavior that is initiated and stopped according to behavioral needs. The timing and sequence of muscle contractions underlying locomotion originate from neuronal networks in the spinal cord called central pattern generators (CPGs; Goulding, 2009; Grillner and Jessell, 2009; Kiehn, 2006). The command for locomotion is integrated in supraspinal centers, which convey the initiating signal to the spinal cord through excitatory reticulospinal neurons of the lower brainstem (Dubuc et al., 2008; Grillner and Georgopoulos, 1996; Jordan et al., 2008; Roberts et al., 2008; Ryczko and Dubuc, 2013). Activity in these neurons is thought to provide the direct activation signal for locomotor CPG networks in all vertebrates. In addition, neural activity related to locomotion is observed in groups of reticulospinal neurons (Deliagina et al., 2000; Drew et al., 1986), suggesting that a sustained descending activity may determine the duration of the locomotor episode. Yet, other studies have indicated that such initiating and maintenance signals may be complemented by a dedicated stop command to allow for a precisely timed locomotor arrest according to behavioral needs. In the *Xenopus* tadpole, head contact with obstacles activates GABAergic descending pathways that immediately terminate swimming (Perrins et al., 2002). Likewise, in the cat, electrical stimulation of the rostral medullary and caudal pontine reticular formations leads to a general motor inhibition (Mori, 1987; Takakusaki et al., 2003).

Excitatory and inhibitory brainstem descending neurons are largely intermingled in the reticular formation (Esposito et al., 2014; Holstege, 1991), which have made it difficult to ascribe locomotor initiating or terminating signals to defined cell populations with standard electrophysiological methods. More recently, developmental genetics has allowed manipulating discrete groups of reticular neurons in mice and addressing their function in motor control (Bouvier et al., 2010; Esposito et al., 2014). In zebrafish caudal-most brainstem V2a neurons, excitatory neurons defined by the expression of the transcription

factor Chx10, have been shown to project to the spinal cord and to participate in the initiation and maintenance of locomotion (Kimura et al., 2013). In mouse, V2a neurons are found in the spinal cord, where they play distinct roles in controlling locomotion (Al-Mosawie et al., 2007; Crone et al., 2008; Crone et al., 2009; Dougherty and Kiehn, 2010; Kiehn, 2011; Lundfald et al., 2007; Zhong et al., 2010), and in the brainstem, where they send descending axons to the spinal cord (Bretzner and Brownstone, 2013; Cepeda-Nieto et al., 2005). In mice, locomotor episodes are associated with the expression of c-*fos*—a biochemical correlate of increased firing—in brainstem V2a neurons (Bretzner and Brownstone, 2013), but no direct link between their activation and locomotor initiation, maintenance, or termination has thus far been described. Here, we functionally evaluate this question in vitro and in vivo and identify a restricted contingent of V2a neurons of the rostral medulla/caudal pons that, upon activation, mediates an immediate arrest of ongoing locomotor activity. V2a "stop neurons" gain their effect via excitatory descending projections to the lumbar ventral spinal cord that may in turn provide an indirect inhibition of the spinal premotor locomotor networks. Our findings thus identify an excitatory functional pathway that favors immobility and thus helps control the episodic nature of locomotion.

RESULTS

V2a Brainstem Neurons Project to the Lumbar Spinal Cord and Are Excitatory

Brainstem V2a neurons were shown to project to the cervical spinal cord (Bretzner and Brownstone, 2013). We thus addressed the possibility that their projections reach the lumbar spinal cord, which contains the networks controlling hindlimb locomotion (Kiehn, 2006). V2a neurons were made permanently detectable by crossing a *Chx10::Cre* mouse line (Azim et al., 2014), which selectively drives Cre recombinase in $Chx10^+$ neurons (Figure S1), with conditional eYFP or Tdtomato lines (hereafter called *Chx10-reporter* mice). Bilateral injections of the retrograde marker Cholera Toxin B (CTB) were targeted to the second lumbar (L2) spinal segment (Figure 1A). CTB^+/Chx10-reporter labeled neurons were detected throughout the medulla and caudal pons and accounted for roughly half of ventrally located, retrogradely labeled neurons. In particular, we considered the fraction of reticulospinal neurons that are V2a at four representative levels (Figures 1B–1E): the caudal pons (caudal pontine reticular nucleus, PnC: 48% ± 4%; n = 4 animals), the rostral and caudal portion of the gigantocellularis nucleus (rGi: 44% ± 4% and cGi: 64% ± 2% respectively), and the reticular formation of the caudal medulla (thereafter referred to as the magnocellular contingent, Mc: 60% ± 5%).

In agreement with previous reports (Al-Mosawie et al., 2007; Bretzner and Brownstone, 2013; Lundfald et al., 2007), we found that almost all V2a neurons express the mRNA for the vesicular glutamate transporter type 2 (Vglut2) regardless of their rostro-caudal or medio-lateral positioning (> 95%, n = 3, Figure 1F) and are thus exclusively excitatory. Additionally, in spite of the medial extension of Chx10-reporter labeling seen in the rostral medulla, we never observed co-expression with serotonergic neurons (Tryptophane Hydroxylase [TPH] positive, 0/584 cells, n = 4 animals, Figure 1G). We next evaluated the possibility for co-expression of inhibitory neurotransmitters within V2a neurons. Overall,

and regardless of their medial or lateral localization, V2a neurons rarely co-expressed GlyT2 (PnC: 5/164 cells, 3%; rGi: 8/258, 3%; cGi: 3/242, 1%; Mc: 2/232, < 1%, n = 2 animals; Figure S2A and S2B) or GAD67 (PnC: 3/347 cells, < 1%; rGi: 2/547, < 1%; cGi: 4/433, < 1%; Mc: 6/406, 1.5%, n = 3 animals; Figures S2C and S2D). Altogether, these data indicate that most if not all V2a brainstem neurons bear a unique glutamatergic phenotype.

Optogenetic Activation of V2a Brainstem Neurons Stops Locomotor-like Activity In Vitro

To address the functional role of V2a neurons in locomotor initiation or termination, we recorded locomotor-like activities by electrophysiologically monitoring flexor-related L2 and extensor related L5 ventral roots in in vitro brainstem-spinal cord preparations of newborn mice (Figure 2). Selective activation of V2a neurons was achieved by expressing the light-activated Channelrhodopsin (ChR2) in $Chx10^{+}$ cells (*Chx10::Cre; R26ChR2*-YFP mice, Hägglund et al., 2013; Figures 2 and S1). To optimally expose reticulospinal neurons to incident light and favor their depolarization, the brainstem was opened along the transverse plane—leading to an "open-book" preparation (Figures 2A and 2B)—and stimulated broadly. Under such conditions, continuous light-activation of brainstem V2a neurons did not induce any detectable changes in ventral root activity when preparations were superfused with normal Ringer solutions (naive preparation; Figure 2B; n > 10).

To test for the possibility that the role of descending V2a neurons may be revealed during ongoing locomotor-like activity, we bath-applied the minimal concentrations of neuroactive substances N-methyl-D-aspartate (NMDA) (5–7 μM) and serotonin (5-HT) (8–10 μM) sufficient to induce slow and intermediate frequency, locomotor-like activity (up to 0.45 Hz; Talpalar et al., 2013; Talpalar and Kiehn, 2010). In those conditions, light-activation of the brainstem V2a neurons induced an immediate stopping of ongoing activity (in 8/9 preparations; Figure 2C). Upon light offset, the activity immediately resumed and the first three to five cycles exhibited a rebound of activity. Similar rebound excitation has been seen after the termination of a hyperpolarization driven by current injection or optogenetic inhibition of spinal interneurons (Dougherty and Kiehn, 2010; Dougherty et al., 2013; Wilson et al., 2005; Zhong et al., 2010), suggesting that spinal locomotor neurons may have undergone synaptic inhibition during light exposure.

We questioned whether the arrest of locomotor-like activity is mediated by the recruitment of an inhibitory descending pathway in the brainstem (Holstege, 1991) or is integrated in the lumbar spinal cord. For this, the perfusion was separated between the brainstem and the spinal cord at the lower thoracic level (T8–T12) using a split-bath. This allowed blocking glutamatergic transmission selectively in the brainstem with 4 mM of kynurenic acid (KYN), known to completely block NMDA and AMPA/Kainate receptors at this concentration (Hägglund et al., 2010; Figure 2D). In those conditions, brain-stem light exposure still induced an arrest of locomotor-like activity followed by a rebound of activity (Figures 2D and 2E). This observation indicates that the descending signal is directly conveyed by descending excitatory V2a brainstem neurons acting through an inhibitory network located in the lower-thoracic or lumbar segments. Both flexor-(L2, n = 8) or extensor-(L5) dominated ventral roots (n = 5, Figure 2D) were similarly abolished. Finally, light-activation of brainstem V2a neurons was efficient in suppressing neuronally evoked

locomotor-like activities (n = 4; Figures 2F and 2G). These findings suggest that a population of brainstem V2a neurons provides a direct signal to the spinal locomotor networks to arrest ongoing locomotor-like activity. We will refer to those cells as “V2a stop neurons.”

V2a Stop Neurons Act at the Rhythm Generating Layer of the Locomotor CPG

Depression of ongoing locomotor-like activity by V2a stop neurons could be mediated by tonic inhibition of the motor neurons or by an action at the premotor neuron levels, including the rhythm and patterning layers.

To differentiate these possibilities, we first probed the V2a effect on lumbar motor neurons by whole-cell recordings in vitro (Figures 3A–3D). In the absence of locomotor activity, most motor neurons (10/16, five preparations) responded to light activations by an increase in the frequency of both inhibitory and excitatory post-synaptic events (Figure S3B). The remaining cells showed increase in only excitatory events (2/16) or no changes (4/16; Figure S3A). For responsive cells, the latency from light onset to the first detectable postsynaptic excitatory and inhibitory event was on average 70 ± 4 ms and 60 ± 9 ms, respectively. Thus, in the absence of locomotor-like activity, V2a neurons may mediate a mixture of excitation and inhibition onto motor neurons. The excitatory nature of brainstem V2a neurons implies that the inhibitory connections to motor neurons are polysynaptic, while the excitatory actions may include both poly- and mono-synaptic connections (Esposito et al., 2014).

We next looked for signs of tonic inhibition of motor neurons in response to V2a activation during locomotor-like activity. When cells were held at intermediate potentials (−40 to −55 mV), most showed rhythmic oscillations of their membrane potential leading to rhythmic spiking. In response to light, motor neurons showed either a complete arrest (n = 4) or a significant reduction (n = 6) in their spiking frequency (Figures 3B and 3C), independently of the type of synaptic inputs observed before the induction of locomotor-like activity (Figure S3A and S3B). This effect was systematically associated with the disappearance of rhythmic membrane oscillations, in contrast to what is observed following the direct hyperpolarization of the cell using current injection, where subthreshold rhythmicity remains (Figure 3B). When cells were recorded in voltage-clamp, light-activation induced a loss of the rhythmic barrages of inhibitory and/or excitatory postsynaptic currents that are normally associated with ongoing locomotor activity (Figure 3D). Together these observations suggest that the arrest of locomotor-like activity does not owe to strong direct inhibition of motor neurons, but that V2a stop neurons may depress premotor circuits.

We thus aimed at discriminating between an effect on the rhythm and/or pattern generating circuitries (Kiehn, 2006; McLean and Dougherty, 2015). Should the effect be primarily on rhythm generation, V2a-driven locomotor arrest is expected to be able to affect the frequency rather than the pattern; i.e., left-right and flexor-extensor coordination. We therefore created conditions where standardized V2a activations did not completely arrest ongoing locomotor-like activity by selectively challenging the spinal cord compartment to higher concentrations of locomotor drugs (NMDA > 8 μM, 5-HT: 9–12 μM). Excitatory synaptic transmission was simultaneously blocked in the brainstem using a split-bath. As reported previously, higher drug concentrations led to higher frequencies of locomotor-like

activities (> 0.45 Hz; Talpalar and Kiehn, 2010). In such conditions, upon light-activation of V2a neurons, most (4/5) preparations did not show a complete arrest but a significant reduction in frequency (76% ± 5% of initial values) and amplitude (74% ± 3%) of locomotor activities (Figures 3E–3G). Therefore, those conditions of high spinal excitability, by presumably preventing a complete locomotor arrest from finite light power, reveal that V2a stop neurons can modulate the frequency and amplitude of locomotor bursts. Importantly, the perturbed frequency was not an integer of the frequency prior to the light exposure (Figure 3G) and thus did not owe to skipped bursts. Moreover, shorter (1–2 s) pulses of light given at the expected occurrence of a locomotor burst caused phase-resetting of locomotor rhythm (Figure 3H). Additionally, neither left-right nor flexor-extensor coordination, the typical manifestations of pattern formation, were significantly modified by light-activation of brainstem V2a neurons (Figure 3I). Finally, mirroring those findings, opto-inhibition of V2a brainstem neurons during drug-evoked locomotor-like activity positively modulates burst frequency and amplitude (Figure S4).

Altogether, the possibility for bidirectional modulation of locomotor frequency with preserved left-right and flexor-extensor coordination indicates that V2a stop neurons act primarily on premotor circuits involved in rhythm generation.

V2a Stop Neurons Reside in the Rostral Medulla and Caudal Pons

To regionally define the implicated V2a population, we sectioned the brainstem transversally at different antero-posterior levels and targeted photo-illuminations to the exposed plane (Figure 4). We performed four successive cuts on the same preparation, from the rostral to the caudal medulla. When the brainstem was sliced near the ponto-medullary junction to expose the PnC (Figure 4B), light activation of descending V2a neurons induced a complete arrest of ongoing locomotor-like activity, similar to that reported in the “open-book” preparations (n = 3). A similar effect was observed when the rostral (Figure 4C; n = 2) or caudal Gi (Figure 4D; n = 2) was left intact and exposed to the light, although a few low amplitude bursts occasionally occurred in the latter conditions. In contrast, after removal of the intermediate medulla, thus exposing the caudal-most descending V2a neurons (Mc), light exposure was unable to detectably modify the frequency or amplitude of ongoing locomotor-like activity (Figure 4E; n = 3). Light activation at any of those segmental levels in the absence of locomotor drugs was unable to elicit locomotor-like or bursting activities in the lumbar ventral roots (data not shown). Those experiments reveal that the stop command may preferentially reside in the rostral Gi and PnC, or alternatively, that a critical number of cells is required for its functional manifestation.

Activation of Brainstem V2a Neurons Halts Locomotion In Vivo

The isolated in vitro preparation from transgenic lines precluded investigations of V2a activations during spontaneous quadrupedal locomotion and a refined anatomical characterization of implicated cells. To address these issues, we aimed for activation of V2a stop neurons locally, in freely-moving animals. We injected a Cre-dependent AAV-DIO-ChR2-mCherry virus bilaterally in the rGi of *Chx10::Cre* animals (Figure S5) and implanted an optical fiber at the midline to allow for bilateral illumination of transfected cells (Figure 5A). In two animals, we collected acute brainstem slices, performed whole-cell recordings

of transfected cells, and verified their functional activation under synaptic isolation (Figure 5B). Three to four weeks following viral transfection, locomotion was tested when animals were moving in a linear corridor (Bellardita and Kiehn, 2015; Talpalar et al., 2013). In this assay, light-activation of transfected V2a neurons in rGi stopped ongoing locomotion (n = 7; Figures 5C–5F; Movie S1). The complete locomotor arrest was on average seen 140 ms from light onset, a period allowing the ongoing step to be completed; i.e., for the dragging feet of the forelimbs and hindlimbs to be placed aligned with the leading feet. Animals thus reach a canonical stopping position with the four feet on the ground (Figure 5C). This was seen independently of the initial locomotor speed and persisted throughout the 400 ms windows of illumination (Figure 5D). Kinematic analysis of the hindlimb joints during locomotion and the stop revealed that the two conditions represent significantly different motor outputs (Figures 5E–5G): the foot was placed in front of the hip during arrest (mean angles in degrees before versus during light stimulation [all comparisons tested with U test for circular data]: 12.5° versus −26.6°, $p < 0.05$), the knee angle was more extended during arrest than locomotion (75.6° versus 101.4°, $p < 0.05$), and the feet were flat during arrest unlike during locomotion (foot: 63° versus 16.8°, $p < 0.05$).

Optical stimulation with yellow light—out of the range for activating ChR2—in the same animal or with blue light in Cre-negative animals did not produce locomotor arrest. Finally in two animals, we targeted V2a neurons of the caudal medulla (Mc). There, light-activation did not lead to locomotor arrest. Therefore, specific activation of rGi V2a neurons in vivo halts quadrupedal locomotion and leads to a characteristic stopping position.

Brainstem V2a Stop Neurons Constrain the Episodic Expression of the Locomotor Behavior

To test whether brainstem V2a stop neurons are involved in the episodic manifestation of the exploratory locomotor behavior, we aimed for selectively blocking their synaptic output using tetanus toxin light-chain (TeLC), which prevents pre-synaptic vesicle fusion at the membrane (Schiavo et al., 1992). We used a Cre-dependent TeLC-coding virus that efficiently blocks action potential-evoked synaptic transmission (AAV-FLEX-eYFP-TeLC; Murray et al., 2011), similarly to what is seen in TeLC transgenic animals (Zhang et al., 2014). Three to fourteen days after TeLC or saline (control group) injections in the rGi (Figure 6A), animals' behavior was monitored continuously for 25 min in an open-field setting. All TeLC-treated animals (n = 8) showed a remarkable increase of overall mobility compared to controls (n = 5; Figure 6B; Movie S2). This bias toward locomotion was manifested by a significant increase in the relative time the animals spent moving (Figure 6C), indicative of a perturbed ability to reach and maintain immobility. Consequently, treated animals traveled for longer distances during the recording sessions (Figure 6D) with a higher average locomotor speed (Figure 6E). The number of stops to the time spent moving in TeLC-treated animals decreased to almost one-fourth of controls (Figure 6F). These effects were also seen in individual animals and developed over time (Figure S6A). Importantly, locomotor kinematic analysis showed that the impaired ability to stop was not due to changes in the overall locomotor capability (Figure S6B).

In sum, those observations suggest that V2a stop neurons may be normally mobilized during exploratory behavior to favor and maintain locomotor arrest and thus regulate the episodic nature of locomotion.

To further characterize the impaired ability for stopping in TeLC-treated animals and relate it to a natural behavior, we developed an assay that reveals natural and predictable stop events in wild-type mice and scored the deficiencies upon TeLC treatment. For this, four obstacles of increasing heights were spaced at regular intervals in a linear corridor. Control animals (n = 6) typically ran over the first obstacle but showed increased stopping probability as they progressed to the following higher obstacles, and most did not overcome the last obstacle (Figures 6G and 6H; Movie S3). The spontaneous locomotor arrest was typically associated with a limb configuration reminiscent of the one evoked by the optogenetic stimulation of V2a stop neurons; i.e., the foot placed in front of the hip, and hindlimbs and forelimbs perpendicular to the body axis (Figure 6G). TeLC-treated animals (n = 8) performed similarly as controls when tested 3 days post-injection but subsequently showed increased inability to stop (Figures 6I and S6C). After 9 days, TeLC-treated animals did no longer stop before the obstacles (Figures 6G–6I, Movie S3). Therefore, blocking synaptic output from V2a neurons dramatically compromised animals' ability to naturally arrest their locomotion.

Brainstem V2a Stop Neurons Terminate in the CPG Area and Contact Inhibitory and Excitatory Neurons in the Spinal Cord

Those experiments suggest that V2a stop neurons in the rGi halt ongoing locomotion and may gain their effect by inhibiting rhythm generating circuits in the spinal cord. To start addressing this issue, we performed anterograde labeling of V2a stop neurons (bilateral injections of AAV-DIO-ChR2-mCherry in the rGi) and followed their axonal termination in the lumbar spinal cord (Figures 7 and S7). We found extensive $mCherry^{+}$ fiber tracts in the lateral and ventral funiculi (Figures 7B and S7B). Lamina VII—where locomotor related neurons have been described (Goulding, 2009; Grillner and Jessell, 2009; Kiehn, 2006; McLean and Dougherty, 2015)—was the most abundantly and densely innervated, followed by laminae VIII and X (Figures 7C and 7D). Innervation was more moderate in lamina IX containing motor neurons and virtually absent from dorsal laminae (I–VI). A comparable innervation pattern was detected at upper (T13-L1–L2), intermediate (L3–L4) and caudal (L5–L6) lumbar segments. We next tested whether V2a descending connectivity shows preferential innervation to excitatory versus inhibitory neurons in ventral (VII to X) laminae. We detected a similar fraction of inhibitory glycinergic (GlyT2-GFP; Figure 7F) and excitatory (Vglut2-GFP; Figure 7G) neurons receiving one or more putative somatic synaptic contacts (Figure 7H). In contrast, most motor neurons showed no putative somatic contacts. Thus, V2a stop neurons may act onto spinal inhibitory circuits both directly and indirectly via excitatory relays.

DISCUSSION

Methodological Considerations

The function of brainstem V2a neurons in locomotor arrest is clearest when analyzed on locomotor-like activity in vitro, and we provide numerous evidences for a functionally analog effect in vivo. Activities recorded in the in vitro rodent preparations at early postnatal stages and their perturbations following experimental interferences were previously shown to reliably forecast the consequences on limbed locomotion at later developmental stages (Andersson et al., 2012; Bellardita and Kiehn, 2015; Crone et al., 2008; Crone et al., 2009; Kullander et al., 2003; Talpalar et al., 2013; Zhang et al., 2014). Here, we extend this reasoning to long-range, descending projections. A potential limit may have resided in the unequal maturity of descending systems in the newborn animal. Nevertheless, the consistency of our in vitro and in vivo observations suggests that V2a descending projections, similar to the caudal glutamatergic (Hägglund et al., 2010) and serotonergic ones (Liu and Jordan, 2005), are functionally established and incorporated in the locomotor network at birth.

A concern that may be raised with optogenetic activation is that over-activation may cause a depolarizing block of the targeted neurons. The consequences of light-activation of ChR2-expressing V2a neurons could therefore be due to a suspension rather than a gain of their functional output. Importantly, all our experiments employed an approach with minimal light intensity, below which no response could be observed. Second, we never observed an initial excitatory signature followed by decreased activity. Third, when the same neuronal population was made to express the inhibitory opsin NpHR, light-exposure produced an acceleration of locomotor-like activity, a finding making it unlikely that the locomotor cessation observed in the ChR2 experiments is due to impaired firing of those neurons. Finally, stopping-deficiencies were seen with non-optogenetic silencing of V2a neurons (TeLC-mediated). Those observations are indicative that our strategy allows for a valid manipulation of V2a neuronal activity.

V2a Stop Neurons Constitute an Excitatory Pathway Optimally Tuned for Locomotor Arrest

The most significant finding reported here is that activation of V2a neurons of the rostral medulla/caudal pons stops ongoing locomotor activity. In accordance with previous reports (Bretzner and Brownstone, 2013; Kimura et al., 2013), we found V2a neurons to be exclusively glutamatergic. They thus represent a unique contingent that diverges from other excitatory descending systems, thought to favor excitability (Dubuc et al., 2008; Hägglund et al., 2010; Perreault and Glover, 2013; Sivertsen et al., 2014). Importantly, our split-bath experiments in vitro indicate that the V2a descending command is integrated in the spinal cord. The dispensable nature of inhibitory reticulospinal neurons for locomotor arrest stands as a major finding considering the abundance of the latter (Esposito et al., 2014; Holstege, 1991). A significant example is that of muscular atonia seen during REM sleep, driven by inhibitory reticulospinal neurons, themselves activated by the glutamatergic sublaterodorsal tegmental nucleus in the pons (SLD; Lu et al., 2006; Luppi et al., 2011). Although the SLD also sends direct excitatory projections to the spinal cord (Vetrivelan et al., 2009), we found it to be non-V2a (Figure 1B). Together with the absence of evident muscular atonia in vivo,

which is due to complete loss of muscle tone (Caggiano et al., 2014; Luppi et al., 2011), those observations exclude a prominent contribution of sleep-related descending pathways in our study. However, we cannot exclude that inhibitory reticulospinal neurons, should they be recruited by V2a stop neurons in the intact animal, may have a subsidiary role in driving locomotor arrest. Finally, our in vivo kinematic analysis suggests that the V2a-driven locomotor arrest differs from the defensive freezing behavior, which retains immobilization through pronounced co-contraction of muscles (Brandão et al., 2008; Yilmaz and Meister, 2013).

Our findings share similarities with works in cats (Takakusaki et al., 2003) where electrical stimulations in the dorsal tegmental field (pons) or lateral Gi evoked locomotor arrest associated with severe decrease in muscle tone due to inhibition of motor neurons. However, the low specificity of the electrical stimulation and the lack of transmitter characterization prevent a clear estimate of the putative overlap. Nevertheless, the functional analogy may point to a phylogenetic-determined system ensuring all forms of locomotion be controlled by a versatile command system with a built-in circuitry dedicated to constrain its termination, and thus its obligatory episodic nature.

Brainstem V2a Stop Neurons Arrest Locomotor Rhythm Generation

We provide strong evidence that the V2a-mediated locomotor arrest is due to a direct depression of premotor circuits, including in particular those governing rhythm generation. First, although activation of V2a brainstem neurons has both excitatory and inhibitory effects on motor neurons in the absence of locomotion, there is no sign of strong tonic inhibition during the locomotor arrest. Second, ongoing locomotor frequency can be modulated without changing left-right or flexor-extensor coordination when increased spinal excitability prevents a complete stop. This is reminiscent to what we reported recently upon selective silencing of candidate rhythm-generating neurons in the isolated spinal cord (Dougherty et al., 2013). The effect on amplitude modulation may be secondary to the effect on rhythm generation and/or imply additional effects on downstream interneurons. Moreover, a selective inhibition of pattern-generating layers has been associated with a quantal slowing of the motor bursts (Feldman and Kam, 2014) and non-resetting deletions (McCrea and Rybak, 2008), two signatures opposite from our findings. Thus, those observations are in line with a primary impact on rhythm generating layers within the locomotor network (Kiehn, 2006; McLean and Dougherty, 2015). This may allow to selectively arrest the behavior while preserving muscle tone.

The most obvious mechanisms imply the recruitment of spinal inhibitory neurons either directly, or indirectly via local excitatory neurons. Although our study did not examine specifically those targets, the dense innervation found in intermediate and ventral laminae is not overlapping with the location of Ia neurons (Hultborn et al., 1976) or Renshaw cells (Alvarez and Fyffe, 2007), making these populations less likely candidates for the inhibition. Lumbar commissural neurons have been shown to receive excitatory inputs from the brainstem (Szokol et al., 2011), but the preserved left-right coordination upon light-stimulation also suggests that these are not main actors in our study. Finally, the manifestation of the locomotor arrest in vivo on both fore- and hindlimbs suggests that V2a

stop neurons innervate both cervical and lumbar segments, as shown with anterograde labeling of transmitter unspecified Gi neurons (Liang et al., 2015).

Previous studies in zebrafish have shown that caudal-most brainstem excitatory V2a neurons initiate and maintain swimming activity (Kimura et al., 2013). In agreement with Bretzner and Brownstone (2013), we were unable to observe any locomotor promoting effects from stimulating the caudal-most brainstem V2a neurons in vitro. However, stimulating broadly all excitatory neurons of the caudal brainstem does initiate episodes of locomotor-like activity (Hägglund et al., 2010). Therefore, brainstem neurons providing a locomotor-initiating signal may be non-V2a in mice, and/or the abundance of V2a stop neurons and fibers may hinder selective manipulation of the putative locomotor-initiating ones. Further investigations using genetic manipulations of projection specific cell types will undoubtedly help tackle this ambiguity.

Behavioral Activation of V2a Stop Neurons

Interestingly, a unique firing pattern that correlates with the offset of swimming has been identified in lamprey reticulospinal neurons (Juvin and Dubuc, 2009). A similar functional signature has not yet been reported in mice. Further recordings taking advantage of the molecular signature described here will rapidly help address this question. Nevertheless, the deficiency in stopping we described upon V2a silencing indicates that those cells may be spontaneously mobilized during exploratory locomotor behavior to arrest it when needed. This descending stop signal may act in parallel to those initiating and controlling the speed of ongoing locomotion. When an active stop is needed the V2a neurons may be brought into action to arrest locomotion while maintaining an optimized posture to avoid collapse.

EXPERIMENTAL PROCEDURES

Mice Lines

All experiments were approved by the local ethical committee. The following transgenic lines were used: *Chx10::Cre* (kindly provided by S. Crone, K. Sharma, L. Zagoraiou, and T.M. Jessell, see Azim et al., (2014), GlyT2-GFP (Zeilhofer et al., 2005), GAD67-GFP (Tamamaki et al., 2003), Rosa26$^{\text{FloxedSTOP-YFP}}$ or Rosa26$^{\text{FloxedSTOP-Tdtomato}}$, *Rosa26-CAG-LSL-eNpHR3.0-EYFP-WPRE*, and *Rosa26-CAG-LSL-ChR2-EYFP-WPRE* (all from the Jackson Laboratories).

Retrograde Labeling and Neurotransmitter Phenotyping

Chx10::Cre mice were crossed with a conditional reporter line (*Rosa26*^{FlxYFP} or *Rosa26*^{FlxTdtomato}) and occasionally with a *GlyT2-GFP* or *GAD67-GFP* line. CTB was injected bilaterally in the L2 spinal segment on 1–2 month old animals. Additional information on the injection procedure, in situ hybridization, immunohistochemistry, and anatomical quantifications are found in the Supplemental Experimental Procedures.

In Vitro Recording of Locomotor-Like Activity and Optogenetics

Pups (0–4 days) were anaesthetized with isoflurane, decerebrated above the ponto-medullary junction (thus preserving the PnC), and the spinal cord and brainstem were isolated in

Ringer solution and transferred to a recording chamber. Locomotor-like activity was recorded with suction electrodes attached to the L2 and/or the L5 lumbar roots as previously reported. NMDA and 5-HT were bath-applied to induce locomotor-like activity. Neuronally evoked locomotor-like activity was elicited by electrical stimulation of the midline in upper cervical segments (Dougherty et al., 2013; Talpalar and Kiehn, 2010). Light from a 100 W Hg lamp was filtered by 450–490 nm or 536–556 nm band-pass filters for ChR2 and eNpHR, respectively, and directed onto the preparation via a 5× objective. Details, including motor neuron recordings, are found in the Supplemental Experimental Procedures.

In Vivo Optogenetic and Genetic Silencing Experiments

Viral Injections and Ferrule Implantation—*Chx10::Cre* animals aged 1–2 months were used, and 600 nl of an AAVDj-EF1a-DIO-hChR2-p2A-mCheery-WRPE or 300 to 700 nl of an AAV1/2-FLEX-TeLC-eYFP-WPRE virus (Murray et al., 2011) were injected in the rGi bilaterally (−6.0 from Bregma, Lat: 0.5, D/V: −4.0). In the same surgery, an optical fiber (200 μm core, 0.22 NA, Thorlabs) held in a 1.25 mm ferrule was implanted medially (depth −3.5 mm).

Optogenetic Stimulations—Light from a 473 nm laser (Optoduet, Ikecool Corporation) was delivered in trains of pulses (Master 8, AMPI) of 10–20 ms pulse duration, 20–40 Hz frequencies, and train durations of 0.5–1 s. The intensity of the laser was set prior to the experiment at the lowest intensity sufficient to stop locomotion (typically 5–30 mW).

Behavioral Tests—For acute optogenetic activations, mice were running spontaneously in a linear corridor (MotoRater, TSE Systems), and the locomotor behavior was recorded as described in Bellardita and Kiehn, (2015). For chronic silencing tests in the open field, mice were placed in a square Plexiglas box (45 × 45 cm); the first 30 min were considered for acclimatization and the next 25 min for the analysis. In a series of silencing experiments, we utilized the linear corridor supplemented with four obstacles of increasing height. Videos were analyzed using scripts written in Matlab (Mathworks) and R (www.r-project.org/). Details are found in the Supplemental Experimental Procedures.

Supplementary Material

Refer to Web version on PubMed Central for supplementary material.

Acknowledgments

We thank K. Sharma (University of Chicago), S. Crone (Cincinnati Children's), L. Zagoraiou, (Academy of Athens), and T.M. Jessell (Columbia University) for the *Chx10-cre* mouse. This work was supported by the Torsten and Ragnar Söderberg's Foundation (O.K.), Swedish Research Council (O.K.), European Research Council (O.K.), NIH R01 NS090919 (O.K.), and Hjärnfonden (O.K.). J.B. was an EMBO fellow. We thank A.C. Westerdahl and P. Löw for extensive genotyping and N. Sleiers for animal breeding in Kiehn lab. We also like to thank R. Diaz Heijtz (Karolinska) for advice on the open field test. The AAV-DIO-hChR2-mCherry virus was a kind gift from K. Deisseroth (Stanford).

References

Al-Mosawie A, Wilson JM, Brownstone RM. Heterogeneity of V2-derived interneurons in the adult mouse spinal cord. Eur J Neurosci. 2007; 26:3003–3015. [PubMed: 18028108]

Alvarez FJ, Fyffe RE. The continuing case for the Renshaw cell. J Physiol. 2007; 584:31–45. [PubMed: 17640932]

Andersson LS, Larhammar M, Memic F, Wootz H, Schwochow D, Rubin CJ, Patra K, Arnason T, Wellbring L, Hjälm G, et al. Mutations in DMRT3 affect locomotion in horses and spinal circuit function in mice. Nature. 2012; 488:642–646. [PubMed: 22932389]

Azim E, Jiang J, Alstermark B, Jessell TM. Skilled reaching relies on a V2a propriospinal internal copy circuit. Nature. 2014; 508:357–363. [PubMed: 24487617]

Bellardita C, Kiehn O. Phenotypic characterization of speed-associated gait changes in mice reveals modular organization of locomotor networks. Curr Biol. 2015; 25:1426–1436. [PubMed: 25959968]

Bouvier J, Thoby-Brisson M, Renier N, Dubreuil V, Ericson J, Champagnat J, Pierani A, Chédotal A, Fortin G. Hindbrain interneurons and axon guidance signaling critical for breathing. Nat Neurosci. 2010; 13:1066–1074. [PubMed: 20680010]

Brandão ML, Zanoveli JM, Ruiz-Martinez RC, Oliveira LC, Landeira-Fernandez J. Different patterns of freezing behavior organized in the periaqueductal gray of rats: association with different types of anxiety. Behav Brain Res. 2008; 188:1–13. [PubMed: 18054397]

Bretzner F, Brownstone RM. Lhx3-Chx10 reticulospinal neurons in locomotor circuits. J Neurosci. 2013; 33:14681–14692. [PubMed: 24027269]

Caggiano V, Sur M, Bizzi E. Rostro-caudal inhibition of hindlimb movements in the spinal cord of mice. PLoS ONE. 2014; 9:e100865. [PubMed: 24963653]

Cepeda-Nieto AC, Pfaff SL, Varela-Echavarría A. Homeodomain transcription factors in the development of subsets of hindbrain reticulospinal neurons. Mol Cell Neurosci. 2005; 28:30–41. [PubMed: 15607939]

Crone SA, Quinlan KA, Zagoraiou L, Droho S, Restrepo CE, Lundfald L, Endo T, Setlak J, Jessell TM, Kiehn O, Sharma K. Genetic ablation of V2a ipsilateral interneurons disrupts left-right locomotor coordination in mammalian spinal cord. Neuron. 2008; 60:70–83. [PubMed: 18940589]

Crone SA, Zhong G, Harris-Warrick R, Sharma K. In mice lacking V2a interneurons, gait depends on speed of locomotion. J Neurosci. 2009; 29:7098–7109. [PubMed: 19474336]

Deliagina TG, Zelenin PV, Fagerstedt P, Grillner S, Orlovsky GN. Activity of reticulospinal neurons during locomotion in the freely behaving lamprey. J Neurophysiol. 2000; 83:853–863. [PubMed: 10669499]

Dougherty KJ, Kiehn O. Firing and cellular properties of V2a interneurons in the rodent spinal cord. J Neurosci. 2010; 30:24–37. [PubMed: 20053884]

Dougherty KJ, Zagoraiou L, Satoh D, Rozani I, Doobar S, Arber S, Jessell TM, Kiehn O. Locomotor rhythm generation linked to the output of spinal shox2 excitatory interneurons. Neuron. 2013; 80:920–933. [PubMed: 24267650]

Drew T, Dubuc R, Rossignol S. Discharge patterns of reticulospinal and other reticular neurons in chronic, unrestrained cats walking on a treadmill. J Neurophysiol. 1986; 55:375–401. [PubMed: 3950696]

Dubuc R, Brocard F, Antri M, Fénelon K, Gariépy JF, Smetana R, Ménard A, Le Ray D, Viana Di Prisco G, Pearlstein E, et al. Initiation of locomotion in lampreys. Brain Res Brain Res Rev. 2008; 57:172–182.

Esposito MS, Capelli P, Arber S. Brainstem nucleus MdV mediates skilled forelimb motor tasks. Nature. 2014; 508:351–356. [PubMed: 24487621]

Feldman JL, Kam K. Facing the challenge of mammalian neural microcircuits: Taking a few breaths may help. J Physiol. 2014

Goulding M. Circuits controlling vertebrate locomotion: moving in a new direction. Nat Rev Neurosci. 2009; 10:507–518. [PubMed: 19543221]

Grillner S, Georgopoulos AP. Neural control. Curr Opin Neurobiol. 1996; 6:741–743. [PubMed: 9000031]

Grillner S, Jessell TM. Measured motion: searching for simplicity in spinal locomotor networks. Curr Opin Neurobiol. 2009; 19:572–586. [PubMed: 19896834]

Hägglund M, Borgius L, Dougherty KJ, Kiehn O. Activation of groups of excitatory neurons in the mammalian spinal cord or hindbrain evokes locomotion. Nat Neurosci. 2010; 13:246–252. [PubMed: 20081850]

Hägglund M, Dougherty KJ, Borgius L, Itohara S, Iwasato T, Kiehn O. Optogenetic dissection reveals multiple rhythmogenic modules underlying locomotion. Proc Natl Acad Sci USA. 2013; 110:11589–11594. [PubMed: 23798384]

Holstege JC. Ultrastructural evidence for GABAergic brain stem projections to spinal motoneurons in the rat. J Neurosci. 1991; 11:159–167. [PubMed: 1702461]

Hultborn H, Illert M, Santini M. Convergence on interneurones mediating the reciprocal Ia inhibition of motoneurones. I. Disynaptic Ia inhibition of Ia inhibitory interneurones. Acta Physiol Scand. 1976; 96:193–201. [PubMed: 1258669]

Jordan LM, Liu J, Hedlund PB, Akay T, Pearson KG. Descending command systems for the initiation of locomotion in mammals. Brain Res Brain Res Rev. 2008; 57:183–191.

Juvin L, Dubuc R. Patterns of activity of reticulospinal neurons during locomotion in lampreys. Soc Neurosci Abstr. 2009

Kiehn O. Locomotor circuits in the mammalian spinal cord. Annu Rev Neurosci. 2006; 29:279–306. [PubMed: 16776587]

Kiehn O. Development and functional organization of spinal locomotor circuits. Curr Opin Neurobiol. 2011; 21:100–109. [PubMed: 20889331]

Kimura Y, Satou C, Fujioka S, Shoji W, Umeda K, Ishizuka T, Yawo H, Higashijima S. Hindbrain V2a neurons in the excitation of spinal locomotor circuits during zebrafish swimming. Curr Biol. 2013; 23:843–849. [PubMed: 23623549]

Kullander K, Butt SJ, Lebret JM, Lundfald L, Restrepo CE, Rydström A, Klein R, Kiehn O. Role of EphA4 and EphrinB3 in local neuronal circuits that control walking. Science. 2003; 299:1889–1892. [PubMed: 12649481]

Liang, H.; Watson, C.; Paxinos, G. Terminations of reticulospinal fibers originating from the gigantocellular reticular formation in the mouse spinal cord. Brain Struct Funct. 2015. Published online on January 30, 2015. http://dx.doi.org/10.1007/s00429-015-0993-z

Liu J, Jordan LM. Stimulation of the parapyramidal region of the neonatal rat brain stem produces locomotor-like activity involving spinal 5-HT7 and 5-HT2A receptors. J Neurophysiol. 2005; 94:1392–1404. [PubMed: 15872068]

Lu J, Sherman D, Devor M, Saper CB. A putative flip-flop switch for control of REM sleep. Nature. 2006; 441:589–594. [PubMed: 16688184]

Lundfald L, Restrepo CE, Butt SJ, Peng CY, Droho S, Endo T, Zeilhofer HU, Sharma K, Kiehn O. Phenotype of V2-derived interneurons and their relationship to the axon guidance molecule EphA4 in the developing mouse spinal cord. Eur J Neurosci. 2007; 26:2989–3002. [PubMed: 18028107]

Luppi PH, Clément O, Sapin E, Gervasoni D, Peyron C, Léger L, Salvert D, Fort P. The neuronal network responsible for paradoxical sleep and its dysfunctions causing narcolepsy and rapid eye movement (REM) behavior disorder. Sleep Med Rev. 2011; 15:153–163. [PubMed: 21115377]

McCrea DA, Rybak IA. Organization of mammalian locomotor rhythm and pattern generation. Brain Res Brain Res Rev. 2008; 57:134–146.

McLean DL, Dougherty KJ. Peeling back the layers of locomotor control in the spinal cord. Curr Opin Neurobiol. 2015; 33:63–70. [PubMed: 25820136]

Mori S. Integration of posture and locomotion in acute decerebrate cats and in awake, freely moving cats. Prog Neurobiol. 1987; 28:161–195. [PubMed: 3544055]

Murray AJ, Sauer JF, Riedel G, McClure C, Ansel L, Cheyne L, Bartos M, Wisden W, Wulff P. Parvalbumin-positive CA1 interneurons are required for spatial working but not for reference memory. Nat Neurosci. 2011; 14:297–299. [PubMed: 21278730]

Perreault MC, Glover JC. Glutamatergic reticulospinal neurons in the mouse: developmental origins, axon projections, and functional connectivity. Ann N Y Acad Sci. 2013; 1279:80–89. [PubMed: 23531005]

Perrins R, Walford A, Roberts A. Sensory activation and role of inhibitory reticulospinal neurons that stop swimming in hatchling frog tadpoles. J Neurosci. 2002; 22:4229–4240. [PubMed: 12019340]

Roberts A, Li WC, Soffe SR, Wolf E. Origin of excitatory drive to a spinal locomotor network. Brain Res Brain Res Rev. 2008; 57:22–28.

Ryczko D, Dubuc R. The multifunctional mesencephalic locomotor region. Curr Pharm Des. 2013; 19:4448–4470. [PubMed: 23360276]

Schiavo G, Benfenati F, Poulain B, Rossetto O, Polverino de Laureto P, DasGupta BR, Montecucco C. Tetanus and botulinum-B neurotoxins block neurotransmitter release by proteolytic cleavage of synaptobrevin. Nature. 1992; 359:832–835. [PubMed: 1331807]

Sivertsen MS, Glover JC, Perreault MC. Organization of pontine reticulospinal inputs to motoneurons controlling axial and limb muscles in the neonatal mouse. J Neurophysiol. 2014; 112:1628–1643. [PubMed: 24944221]

Szokol K, Glover JC, Perreault MC. Organization of functional synaptic connections between medullary reticulospinal neurons and lumbar descending commissural interneurons in the neonatal mouse. J Neurosci. 2011; 31:4731–4742. [PubMed: 21430172]

Takakusaki K, Kohyama J, Matsuyama K. Medullary reticulospinal tract mediating a generalized motor inhibition in cats: III. Functional organization of spinal interneurons in the lower lumbar segments. Neuroscience. 2003; 121:731–746. [PubMed: 14568032]

Talpalar AE, Kiehn O. Glutamatergic mechanisms for speed control and network operation in the rodent locomotor CpG. Front Neural Circuits. 2010; 4:4. [PubMed: 20300468]

Talpalar AE, Bouvier J, Borgius L, Fortin G, Pierani A, Kiehn O. Dual-mode operation of neuronal networks involved in left-right alternation. Nature. 2013; 500:85–88. [PubMed: 23812590]

Tamamaki N, Yanagawa Y, Tomioka R, Miyazaki J, Obata K, Kaneko T. Green fluorescent protein expression and colocalization with calretinin, parvalbumin, and somatostatin in the GAD67-GFP knock-in mouse. J Comp Neurol. 2003; 467:60–79. [PubMed: 14574680]

Vetrivelan R, Fuller PM, Tong Q, Lu J. Medullary circuitry regulating rapid eye movement sleep and motor atonia. J Neurosci. 2009; 29:9361–9369. [PubMed: 19625526]

Wilson JM, Hartley R, Maxwell DJ, Todd AJ, Lieberam I, Kaltschmidt JA, Yoshida Y, Jessell TM, Brownstone RM. Conditional rhythmicity of ventral spinal interneurons defined by expression of the Hb9 homeodomain protein. J Neurosci. 2005; 25:5710–5719. [PubMed: 15958737]

Yilmaz M, Meister M. Rapid innate defensive responses of mice to looming visual stimuli. Curr Biol. 2013; 23:2011–2015. [PubMed: 24120636]

Zeilhofer HU, Studler B, Arabadzisz D, Schweizer C, Ahmadi S, Layh B, Bösl MR, Fritschy JM. Glycinergic neurons expressing enhanced green fluorescent protein in bacterial artificial chromosome transgenic mice. J Comp Neurol. 2005; 482:123–141. [PubMed: 15611994]

Zhang J, Lanuza GM, Britz O, Wang Z, Siembab VC, Zhang Y, Velasquez T, Alvarez FJ, Frank E, Goulding M. V1 and v2b interneurons secure the alternating flexor-extensor motor activity mice require for limbed locomotion. Neuron. 2014; 82:138–150. [PubMed: 24698273]

Zhong G, Droho S, Crone SA, Dietz S, Kwan AC, Webb WW, Sharma K, Harris-Warrick RM. Electrophysiological characterization of V2a interneurons and their locomotor-related activity in the neonatal mouse spinal cord. J Neurosci. 2010; 30:170–182. [PubMed: 20053899]

Highlights

- Mouse V2a brainstem neurons are excitatory and project to the ventral spinal cord
- Optogenetic activation of V2a neurons of the rostral medulla halts locomotion
- These “V2a stop neurons” act by depressing locomotor rhythm generation
- V2a stop neurons are needed for episodic locomotion

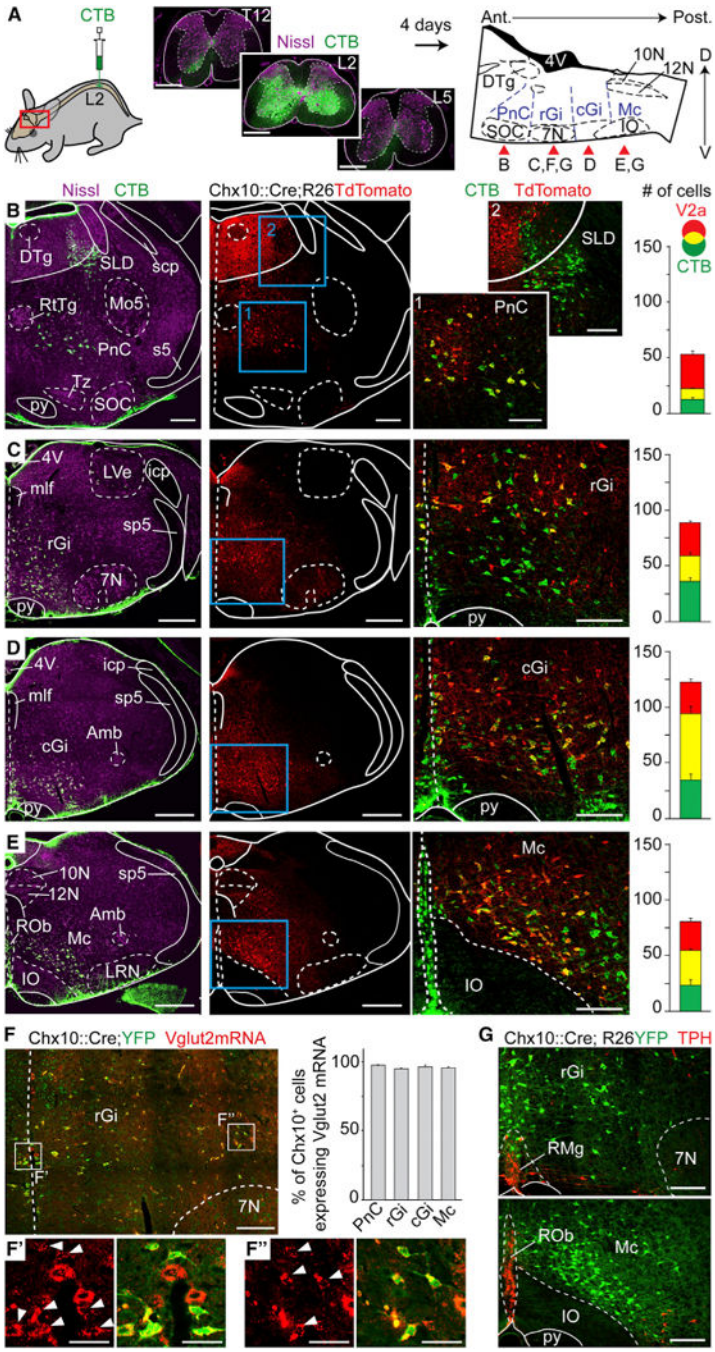

Figure 1. V2a Brainstem Neurons Project to the Lumbar Spinal Cord and Are Excitatory

(A) Bilateral injections of the retrograde marker CTB at the 2nd lumbar segment of the spinal cord (left). To the right is a sagittal schematic of the brainstem indicating the approximate rostrocaudal levels shown in the specified panels (red arrows) where CTB-labeled neurons are detected.

(B–E) Transverse hemi-sections at the levels indicated in (A) stained for CTB, Nissl, and V2a neurons (Tdtomato). Right-most pictures are magnifications of the blue boxed area;

V2a reticulospinal neurons appear yellow. Bar-graphs show the average number of CTB, V2a, and double-labeled neurons per hemisection (n = 4 animals). Error bars are SEM.
(F) Transverse hemi-section in the rGi indicating Vglut2$^+$ glutamatergic (red) V2a neurons (YFP). Bar-graphs show the average percentage of Vglut2$^+$;V2a neurons (n = 3 animals). Insets in F′ and F″ are magnified views of Vglut2 expression alone (left) and merged with YFP (right) of medially-(F′) and laterally positioned (F″) V2a neurons. White arrowheads indicate co-expression. Error bars are SEM.
(G) Transverse hemi-sections stained for TPH and V2a neurons (YFP). Note the absence of co-expression (n = 4 animals).
Scale bars (in μm): (A): 500, low magnifications in (B)–(E): 500; magnified views in (B)–(G): 200; F′ and F″: 50. Abbreviations used in all figures: 10N: dorsal motor nucleus of vagus; 12N: hypoglossal nucleus; 4V: 4th ventricle; 7N: facial nucleus; Amb: ambiguus nucleus; Gi: gigantocellular reticular nucleus; GiA: gigantocellular reticular nucleus alpha part; icp: inferior cerebellar peduncle; IO: Inferior olive; DTg: laterodorsal tegmental nucleus; LRN: lateral reticular nucleus; LVe: lateral vestibular nucleus; Mc: magnocellular reticular nucleus; mlf: medial longitudinal fasciculus; Mo5: motor trigeminal nucleus; PnC: caudal pontine reticular nucleus; py: pyramidal tract; ROb: raphe obscurus nucleus; RMg: raphe magnus nucleus; RtTg: reticulotegmental nucleus of the pons; s5: sensory root of the trigeminal nerve; scp: superior cerebellar peduncle; SLD: Sublaterodorsal tegmentum; SOC: Superior olivary complex; sp5: spinal trigeminal tract; Tz: nucleus of the trapezoid body. See also Figure S2.

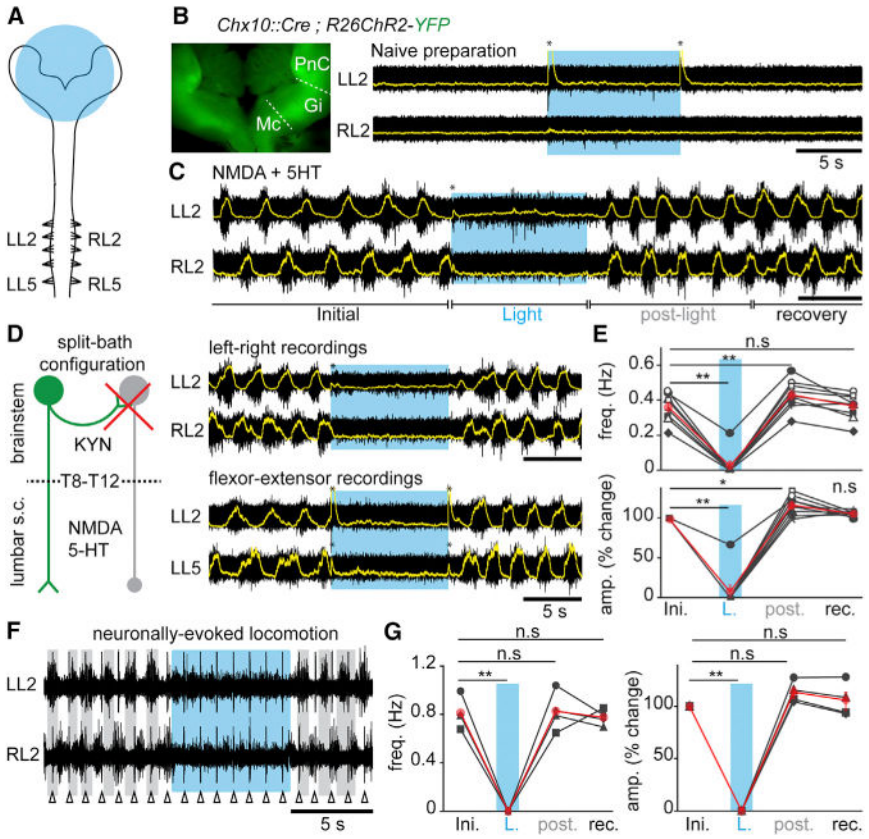

Figure 2. V2a Brainstem Neurons Stop Slow-Frequency Locomotor-like Activity In Vitro

(A) Schematic experimental design for electrophysiological recordings in brainstem-spinal cord preparations from postnatal animals (0–4 days). The area of light stimulation is shown in blue.

(B) Inset: ChR2-YFP expression in the “open-book” brainstem preparation. Raw (black) and integrated signals (superimposed in yellow) of L2 ventral roots in normal Ringer solution. Light-activation of brainstem V2a neurons (blue epoch) does not change baseline activity. The transient voltage deflections at light onset and offset (asterisks) are light-mediated artifacts.

(C) Similar recordings during locomotor-like activity induced with 5–7 μM NMDA and 8 μM 5-HT. Light-activation of brainstem V2a neurons stops ongoing locomotor-like activity.

(D) Left: the possible recruitment by V2a neurons (green) of other inhibitory descending neurons (gray) was blocked by applying KYN onto the brainstem in a split-bath configuration. Right: recordings of the flexor-dominated roots bilaterally (L2, top) and of flexor and extensor (L5)-dominated roots on the same side (bottom).

(E) Average per animal (black, n = 9) and grand average among animals (red) of the instantaneous frequency and of the percent change in amplitude of drug-evoked locomotor bursts before (Initial: ini.), during light (L.), for 5 cycles following light offset (post), and for the following 20 s (recovery: rec).

(F) Recordings of L2 roots bilaterally in the split-bath configuration during electrical stimulation (1Hz, Δ) at the first cervical segment. Vertical lines are stimulus artifacts.

(G) Average per animal (black, n = 4) and grand-average among animals (red) of the instantaneous frequency and of the percent change in amplitude of descending fiber evoked locomotor bursts.

In all panels: n.s. indicates non-significant, * indicates $p < 0.05$ and ** indicates $p < 0.01$ (paired t test); Error bars in (E) and (G) are SEM.

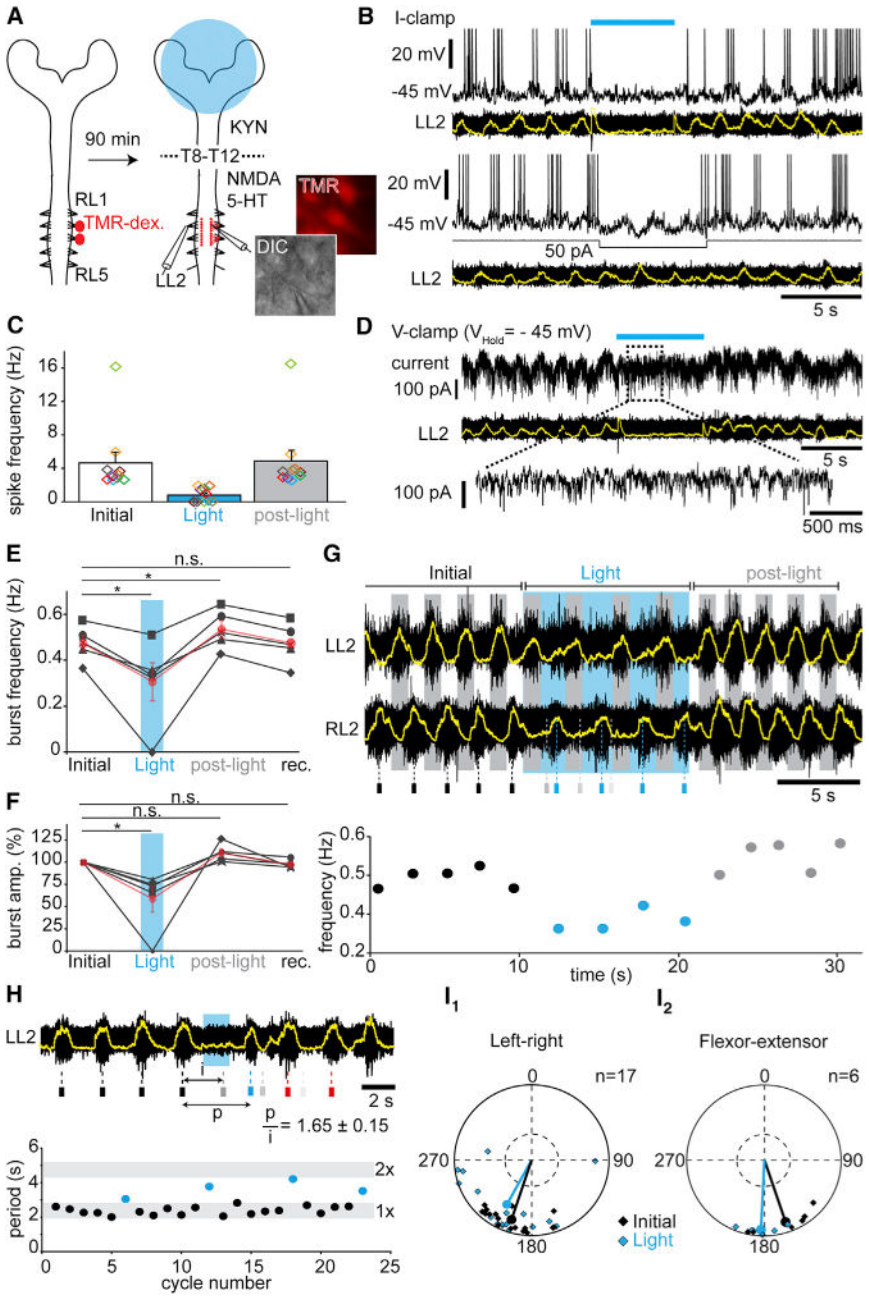

Figure 3. Light-Activation of Brainstem V2a Neurons Depresses Rhythm-Generating Levels of the Locomotor CPG

(A) Experimental design for labeling and whole-cell recording of lumbar motor neurons. TMR-dex: Tetramethyl-Rhodamine Dextran.

(B) L2 motor neuron in current-clamp during drug-evoked locomotor-like activity. V2a neurons' activation (blue bar) arrests both spiking and underlying membrane oscillations (top), while direct hyperpolarization of the same cell with current injection (bottom) preserves subthreshold oscillations.

(C) Average per cell (colored rectangles, n = 10) and grand-average among cells (bar-graphs) of the instantaneous spiking frequencies of lumbar motor neurons before (initial), during (Light) and after (post-light) light-activation.
(D) Same cell as in (B) recorded in voltage-clamp. Light-activation induces a loss of rhythmic currents.
(E–F) Average per animal (n = 5) and grand-average among animals (red) of the instantaneous frequency (E) and of the percent changes in amplitude (F) of L2 locomotor bursts on preparations facing high NMDA concentrations (> 8 μM). * indicates $p < 0.05$ (paired t test).
(G) Typical L2 ventral root recording during high-frequency locomotor-like activity (~0.5 Hz). Small rectangles below indicate the time of peak of the control RL2 bursts (black), and their forecasted (gray) and actual occurrences (blue) during light activation of brainstem V2a neurons, showing a non-graded slowing of the rhythm. Below is plotted the corresponding instantaneous frequency of RL2 bursts.
(H) L2 ventral root recording during drug-evoked locomotor-like activity. The expected burst is silenced (gray bar below) and the rhythm reset by short light-pulse, as seen by the perturbed period (p) not falling in the range of twice the initial period (i). The graph below illustrates initial (black) and perturbed periods (blue) for four consecutive trials.
(I) Circular plot showing the left-right (I_1) or flexor-extensor (I_2) phase-relationships for individual trials and for the mean preferred phase among all trials before (Initial, black) and during (Light, blue) light-activation. Phase values falling in the bottom-half of the outer circles indicate alternation. There is no significant difference between control and light conditions (Watson-William's test $p > 0.05$). See also Figure S3 and S4.
Error bars in (C), (E), and (F) are SEM.

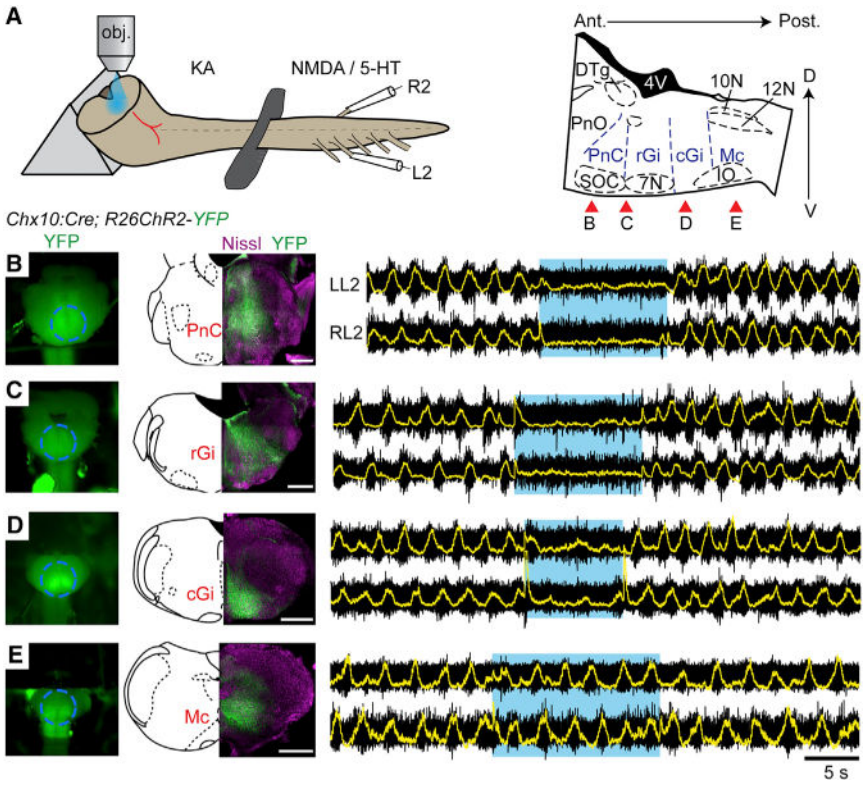

Figure 4. V2a Stop Neurons Reside in the Rostral Gigantocellularis and Caudal Pontine Reticular Nuclei

(A) Experimental set-up. The brainstem is sectioned transversally to expose a given transverse plane to the light. Red arrows on the right indicate approximate levels of the sections performed in (B)–(E).

(B–E) Simultaneous electrophysiological recordings of L2 roots on either side after a section exposing the PnC (B) and of the same preparation after having removed the PnC (C), and the rGi (D) or cGi (E). The ability of light stimulation to stop ongoing locomotion is lost when only the caudal-most medullary formation remains. The transient voltage deflections visible on the integrated traces at light onset and offset are light-mediated artifacts.

Scale bar, 500 μm

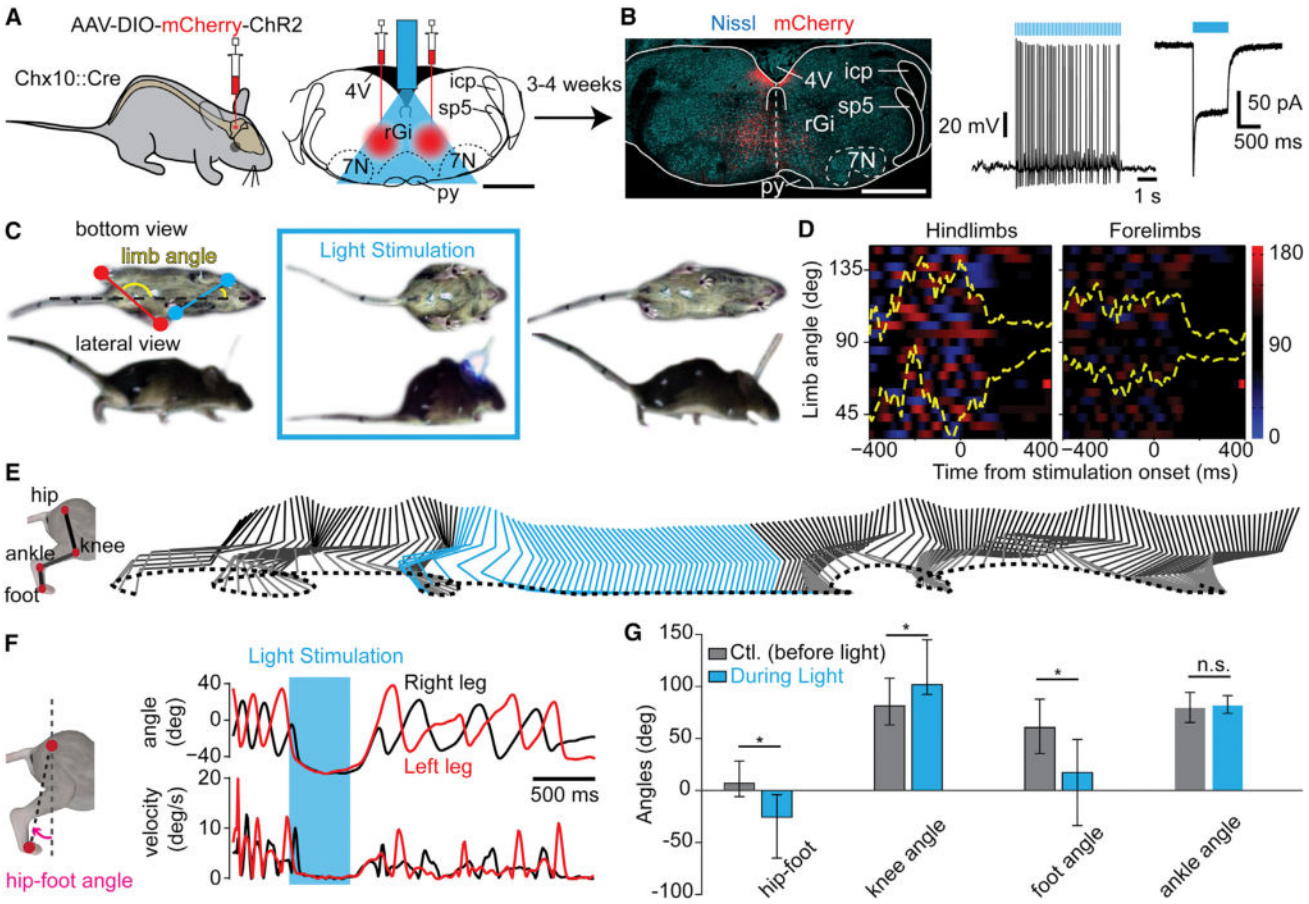

Figure 5. Optogenetic Activation of Brainstem V2a Neurons Halts Locomotion in Freely-Moving Mice

(A) Scaled reconstruction of the implantation and illumination range following the bilateral viral injection in the rGi.

(B) Transverse section showing mCherry expression (red) at the injection site. To the right is a mCherry^{+} neuron recorded in a transverse slice under synaptic isolation.

(C) Detoured snapshots of a freely-moving *Chx10::Cre* mouse 4 weeks post-injection before (left), during (center), and after (right) light-stimulation using pulsed blue light. The limb angle is defined as the angle between a line joining the two hindpaws (red) or forepaws (blue), with respect to the midline of the animal.

(D) Color plot of hindlimbs' and forelimbs' angles 400 ms before and after light onset. The y axis represents 23 trials from seven animals. A gradient of color to red indicates positive angle (left limb behind the right limb), to blue indicates the reverse (right limb behind left limb), and black indicates perpendicular limbs to the body axis. In yellow are shown the 25 and 75 percentile of the distribution of the angle oscillations over time. Independently of the speed before stimulation, light activation of transfected V2a neurons stopped ongoing locomotion and animals remained in a stereotypical position with the limb perpendicular to the body axis (90°).

(E) Kinematic representation of the relative movements of the hip, knee, ankle, and foot of one animal before (gray) and during (blue) light activation. Movements stopped in response to light and resumed upon light offset.

(F) Evolution of the hip-foot angle (pink) as a function of time (top) and corresponding relative velocities (bottom). Light-activation led to a configuration where the foot was kept ahead of the hip.

(G) Average (n = 7 mice) of the hip-foot, knee, foot, and ankle angles 400 ms before (gray) and during (blue, from 100 ms to 500 ms after light onset) light-activation of V2a neurons. Asterisks indicate significant different values ($p < 0.05$, U test for circular data).

Error bars are 25–75 percentiles. Scale bar, 1 mm (A, B). See also Figure S5.

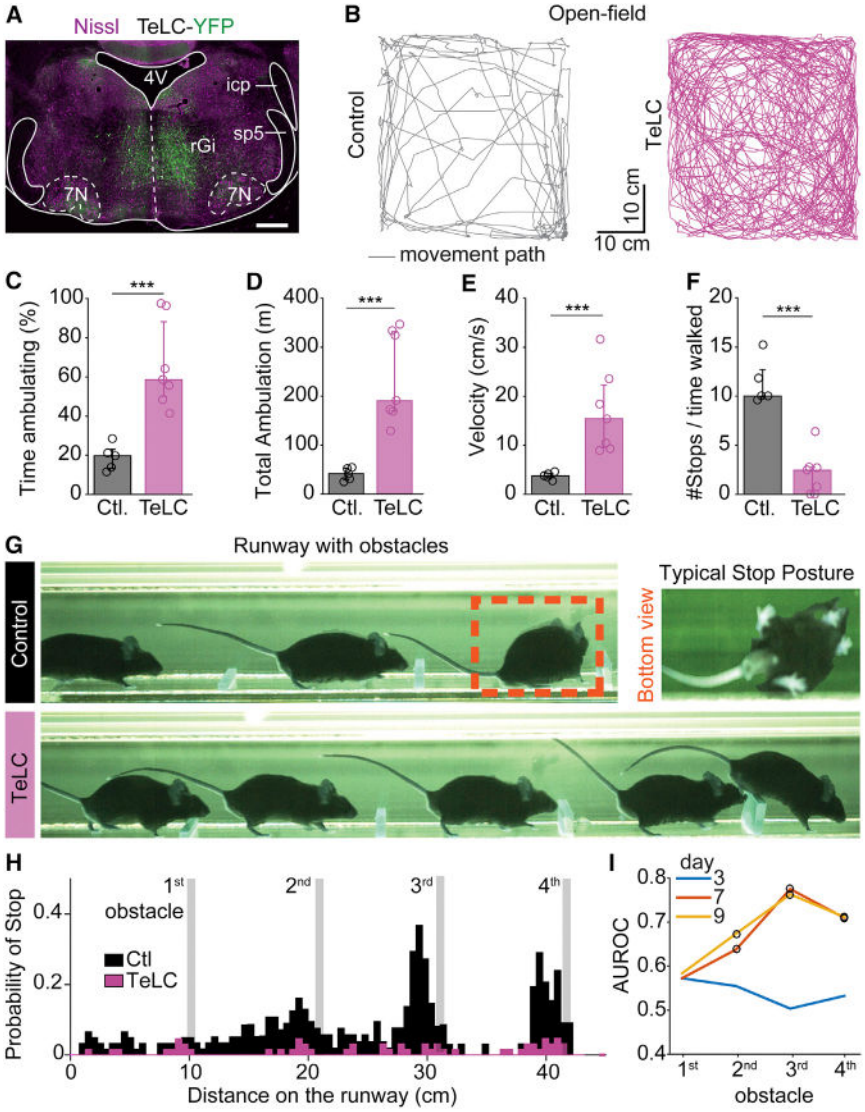

Figure 6. Blocking Synaptic Output from V2a Stop Neurons Increases Mobility

(A) Transverse brainstem section showing the expression of an AAV1/2-FLEX-TeLC-eYFP-WPRE virus following injection in the rGi bilaterally in a *Chx10::Cre* animal.

(B) Traces of movements for 10 min in an open field test 7 days after the injection of saline (control, left) or the TeLC virus (right).

(C) Averages from individual animals (open circles) and grand-average among all individuals (bargraphs) of the percent time spent ambulating for controls (gray, n = 5) and TeLC-treated (pink, n = 8) subjects. Error bars are 25–75 percentiles. In all panels *** indicates $p < 0.005$ (U test).

(D–F) Similar quantifications for (D) the total distance achieved while ambulating, (E) the average velocity of ambulation, and (F) the relative number of stops to the time spent ambulating.

(G) Snapshots of a *Chx10::Cre* mouse 9 days post-injection of saline (control, top) or TeLC virus (bottom) in the rGi. The control animal shown spontaneously halts before the 3rd

obstacle and adopts a stereotypical stopping position, while the TeLC-treated animal does not stop at any obstacle (see also Movie S3).

(H) Summary of the probability of stop for saline-(n = 6, black) or TeLC-injected (n = 8, pink) mice, after 9 days. Controls stopped with higher probability on the 3rd and 4th obstacles ($p < 0.05$, Kruskal-Wallis, Bonferroni correction for multiple comparisons) than TeLC-treated animals.

(I) Direct comparison of the probability of stop before each obstacle between controls and TeLC mice. AUROC index gauges the difference between conditions where 0.5 indicates no difference while values toward zero or one indicate that the probability curves are different. Circles indicate significant differences ($p < 0.05$). See also Figure S6.

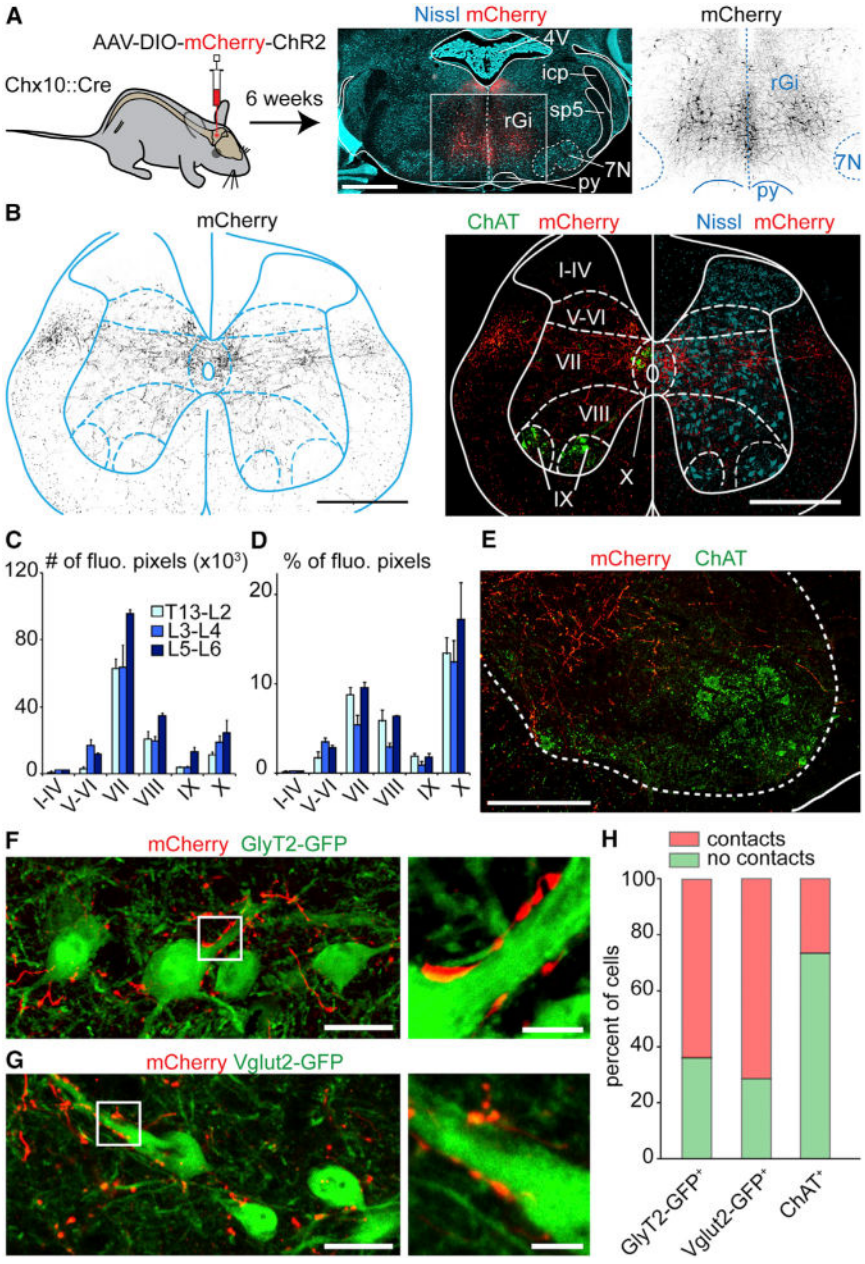

Figure 7. V2a Stop Neurons Terminate Predominantly in Lamina VII of the Lumbar Spinal Cord

(A) Bilateral injections of a Cre-dependent AAV-hChR2-mCherry-virus (middle: red; right: black) in the rGi of *Chx10::Cre* animals.

(B) Transverse L2 spinal cord section of the same animal showing transfected V2a processes (black on the left, red on the right). Rexed's laminae are delineated using ChAT and Nissl staining.

(C–D) Quantification in one animal of the number (C) or the percent (D) of fluorescent pixels in each lamina at the upper (T13-L1-L2), intermediate (L3–L4), and caudal (L5–L6) lumbar levels.

(E) Magnified view of the descending V2a innervation (red) in the vicinity of $ChAT^+$ motor neurons (green).
(F, G) Similar anterograde labelings on a *Chx10: :Cre; GlyT2-GFP* (E) or *Chx10: :Cre; Vglut2-GFP* animal (F) showing putative V2a contacts (red) onto glycinergic and glutamatergic neurons, respectively.
(H) Percent of glycinergic (232 cells), glutamatergic (105 cells), and motor neurons somatas (124 cells) exhibiting no (green) or more than one (red) putative V2a contact.
Scale bars (in μm): (A): 1000, (B): 500, (E): 200, (F, G): 25, insets in (F,G): 5; Error bars in (C) and (D) are SEM; See also Figure S7.